Spatial and Temporal Coincidence Measurement on a Metasurface in Low Light Regime

Randy Stefan Tanuwijaya,* Tsz Kit Yung,† and Jensen T.H. Li‡
Department of Physics
The Hong Kong University of Science and Technology
Clear Water Bay, Hong Kong
(Dated: August 27, 2021)

The optical metasurface has been shown to manipulate photons with minimal loss while maintaining their quantum mechanical properties. We demonstrate the use of a 32 × 32 pixel time correlated single-photon counting (TCSPC) single-photon avalanche diode (SPAD) camera to measure the spatial and temporal coincidence distribution of photons in low light regime. The main challenge posed in the data analysis is to extract true coincidence from measured coincidence which are highly contaminated by accidental coincidence due to the limitations of our SPAD cameras having multiple cycles per frame. Furthermore, we propose a fully vectorized algorithm for measuring the spatial and temporal distribution of coincidence photons and constructed a model to extract the true coincidence of the contaminated measured coincidence. In addition, we experimentally demonstrated the two-photons interference using the optical metasurface and verify the Hong-Ou-Mendel (HOM) dip from the true coincidence predicted by our model. At the end, we also discuss some issues with the current model and proposed future work on this project.

I. INTRODUCTION

Optical metamaterials have shown several exceptional features those are not possible with natural material, such as negative refractive index [1], super lens [2], and invisibility cloak [3]. Although metamaterial can produce such interesting properties, the thickness of the metamaterial has leads to the extensive loss and causes a lot of challenge in the nanofabrication. Due to such limitations, development of optical metasurface, a thin metamaterial with subwavelength thickness, has emerged in recent years to manipulate the properties of the incident photons with minimal loss. On the other hand, the recent emerge of the Time-Correlated Single-Photon-Counting (TCSPC) Single Photon Avalanche Diode (SPAD) camera allows spatial and temporal imaging of quantum optical properties of each individual photons, such as the coincidence detection of photon pairs [4], and space-momentum entanglement of the photon [5]. Furthermore, array of SPADs with its high temporal resolution has been previously utilized other fields of optics, such as fluorescence lifetime imaging [6], imaging through scattering media [7], imaging light in flight [8].

On the previous report [9], we have shown the capabilities of the TCSPC technique and coincidence counting to measure the speed of light and to calibrate our experimental setup. Now, we are utilizing the 32-by-32 pixels SPAD camera to reproduce the two-photons interference or HOM effect at a metasurface sample in the low light regime. In this report, we will focus on two aspects of the coincidence, which are the **spatial** and **temporal** distribution.

We proposed a fully vectorized algorithm to map both spatial and temporal coincidence distribution among the camera pixels. This technique is particularly useful in order to measure how each pixels correlates with other pixels. For example, suppose when we define two spots on the camera, we can observe how the **self coincidence** (a pixel with its spot) and **cross coincidence** (a pixel with the other spot) changes when the two-photons interference effect is present.

To investigate the **temporal distribution** of the coincidence, we built a model to fit the measured coincidence and to extract the the true coincidence out of the highly contaminated measured coincidence. The measured coincidence is contaminated with the accidental coincidence because each camera frame is consisted of many cycles, in which a measured coincidence can be caused by a photon pair coming from different laser pulse, but arrives at the same camera frame. The **true coincidence** and **accidental coincidence** are defined as the coincidence of two photons coming from the same laser pulse and different laser laser pulse, respectively.

II. METHODOLOGY

A. Vectorized Algorithm for Mapping Spatial and Temporal Distribution of Coincidence

Our SPAD camera generates a large amount of data for each measurement. One way to optimize the data analysis is by utilizing a vectorized implementation, since vectorized algorithm can has performance benefit from multithreading, thus allowing the calculation to be processed faster. Another important thing to note is the sparsity of the data. There are some methods that allows the sparse matrix to be stored and computed more efficiently compared to a dense matrix. This part will briefly describe

* rstanuwijaya@connect.ust.hk
† tkyungaa@connect.ust.hk, postgraduate supervisor
‡ jensenli@ust.hk, faculty supervisor

the method we used to analyze the data.

Suppose we use 250 ms acquisition time and 5 µs frame time. The number of frames is: $250\,\text{ms}/5\,\mu\text{s} = 50000$ frames. First, the data of the 32×32 SPAD camera comes in a format of '.txt', *txt_data*, with dimensions of $(50000, 32*32)$. This format follows a general rule, where each line denotes a frame and contains the reverse time tag of photon detection within the frame with range of $[0, 1024)$ and 0 denotes no detection. The mechanism of time tagging has been discussed in the previous report [9]. An important thing to note is the matrix has a high sparsity ($> 90\%$) because of the low light condition of the experiment. First we can convert this data to sparse matrix representation to . This allows us to read and parse the data significantly faster in the future run. Then we define the *raw_data* as the *txt_data* reshaped into 3d-matrix, with dimensions of $(50000, 32, 32)$.

Second step is to fix the data with the pixel jitting time and to drop all bad pixels. That is, we subtract all nonzero entries in the raw data with the jitting time for each particular pixel and set the entries for all bad pixels to be zero. Then we store the result as $adjusted\_data = raw\_data - jitter\_time$.

Then, we define two separate spots we are interested on the $adjusted\_data$, namely L' and R' with size of (L_y, L_x) and (R_y, R_x) and flatten it to be 1D vector L and R with size of $(L_x L_y)$ and $(R_x R_y)$. Then we define Time Difference Matrix T, a matrix with size of $(R_x R_y, L_x L_y)$, where:

$$T[i][j] = \begin{cases} L[i] = R[j] & \text{if } L[i] \neq 0 \text{ and } R[i] \neq 0 \\ \infty & \text{otherwise} \end{cases}$$

Define the coincidence window $t_c c > 0$ as the time window (in time bin) in which the coincidence will be counted, and coincidence matrix C (2D Boolean matrix) with the same size as T, where:

$$C[i][j] = \begin{cases} 1 & \text{if } |T[i][j]| \leq t_{cc}/2 \\ 0 & \text{otherwise} \end{cases}$$

Moreover, we can also count the number of measured coincidence at time difference τ. Let $N(\tau)$ be the number of photon arrival with the time difference of $\tau \in [-1024, 1024]$. Note that this measured coincidence $N(\tau)$ is the sum of true coincidence $N_{CC}(\tau)$ and the accidental coincidence $N_{AC}(\tau)$. The source of the accidental coincidence is from the camera having multiple cycles in a single frame and will be elaborated later in the III. Then, $N(\tau)$ is defined as:

$$N(\tau) = \sum_{i,j} \left(T[i][j] - \tau\right)$$

Where denotes the logical NOT operator, i.e. $(0) = 1$ and not $(x \neq 0) = 0$.

Now suppose we are interested to count the number of the coincidence for each pixel or to plot the coincidence

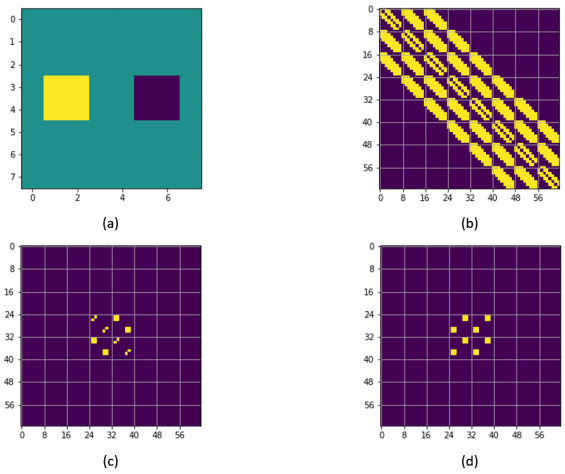

FIG. 1. F-matrix for 8x8 pixels camera (a) The two 2x2 spots, (b) F-matrix for nearby pixels with radius of 2 pixels, (c) F-matrix for self-coincidence, (d) F-matrix for cross-coincidence

distributions. This time consider the special case when the two regions all the pixels, i.e $L = R = A$, with the size of $(32, 32)$. Note some unique features of the Time Difference matrix T and the Coincidence Matrix C. T matrix is inversely symmetric across the diagonal, and the diagonal entries will be 0 or ∞ as $T[i][i] = A[i] - A[i] = 0$ and C matrix is symmetric across the diagonal. Also note that the size of T and C matrix is $(1024, 1024)$.

We define F matrix or the filter matrix, which is to determine which how each pixel correlates with each other. The F matrix is a mask to filter out the C matrix that we are not interested in. For example, suppose we divide the pixels into two regions with equal size (left and right spots). We can create a F matrix to only count **self coincidence** (left-left and right-right), or to count the **cross coincidence** (left-right). We can also create a F matrix to only count the coincidence with the neighboring pixels with a certain radius. Also note that $F[i][i]$ must be 0 because a pixel cannot be correlated with itself. The definition of F matrix is simple, but the implementation is different according to our need. Some F-matrix examples are shown in Fig 1

Define filtered coincidence matrix C' as:

$$C'[i][j] = C[i][j] \& F[i][j]$$

Where & is the logical AND operator. Also note that C' is symmetric. Finally, to get the coincidence of each pixel, we need to sum C' along any axis, and reshape it back to (32, 32) and sum it for all frames. Let the number of measured coincidence for pixel i as the result array $M[i]$. The result M array is given by:

$$M[i] = \sum_j C'[i][j]$$

B. Model for Temporal Distribution of Measured Coincidence

As previously discussed, the measured coincidence is highly contaminated with the accidental coincidence because of the camera having many cycles per frame. Our SPAD camera has multiple cycles N per frames, where $N = 100$. The measured coincidence from our algorithm $N(\tau)$ is the sum of both true and accidental coincidence. The two photons interference only occurs on the true coincidence, where the photon pairs are coming from the same laser pulse. Therefore, we propose a model to decompose the measured coincidence $N(\tau)$ into true coincidence $N_{CC}(\tau)$ and accidental coincidence $N_{AC}(\tau)$.

First, consider a laser pulse with a Lorentzian distribution in time with amplitude A and FWHM t_w:

$$E(t) = \frac{A}{\pi(t_w/2)}\left[\frac{(t_w/2)^2}{t^2 + (t_w/2)^2}\right]$$

The distribution of the two photon pulses on two different pixels $\Delta E_k(\tau)$ is given by the convolution of two individual pulse $E(t)$, assume $t_1 - t_2 = k\Delta T$, where k is the number of cycle difference between the frist and second photons and ΔT is the jitting time per cycle.

$$\begin{aligned}\Delta E_k(\tau) &= \int_{-\infty}^{\infty} E_1(t - t_1)E(t - t_2 - \tau)dt \\ &= A_1A_2\frac{1}{\pi t_w}\left[\frac{t_w^2}{(\tau - k\Delta t)^2 + t_w^2}\right]\end{aligned}$$

The SPAD camera only records the time arrival of the first photon in any of the cycle within the frame. Suppose the probability of detection in a pixel is $\eta << 1$ (low light assumption) and the laser follows a Poisson distribution with parameter m. We purposely make the camera and the laser out of sync with a jitting time per cycle of ΔT to distinguish the true coincidence from the accidental coincidence. The probability of two photons arriving from the same cycle (true coincidence) is:

$$\begin{aligned}P(\tau = 0) &= \sum_{j=1}^{N} \eta^2(1-\eta)^{2(j-1)} \left\langle A_j^2 \right\rangle \\ &\approx m(m+1)N\eta^2\end{aligned}$$

On the other hand, the probability of two photons arriving from k cycles apart is (accidental coincidence) is given by:

$$\begin{aligned}P(\tau = k\Delta T) &= \sum_{j=1}^{N-|k|} \eta^2(1-\eta)^{2(j-1)+|k|} \left\langle A_j A_{j+k} \right\rangle \\ &\approx m^2(N - |k|)\eta^2\end{aligned}$$

Then, assuming that the camera has Z time bins, the total probability for a pair of photons arrives with time difference τ is:

$$f(\tau) = \frac{Z - \tau}{Z}$$

We further consider the aliasing effect, where two photons from k pulse apart arrives at $k \pm 1$ cycles apart. IN this case, the measured time difference would be $\tau - Z$ or $\tau + Z$ instead of τ. Let the expected number of coincidence at with time difference τ is given by $g(\tau)$, where:

$$g_k(\tau) = \int_{\tau - t_{CC}/2}^{\tau + t_{CC}/2} \Delta E(\tau)\, dt = \arctan\left(\frac{\tau - k\Delta T + t_{cc}/2}{t_w}\right)$$

We construct the model for the number of true and accidental coincidence $N_{CC}(\tau)$ and $N_{AC}(\tau)$ with t_{CC} coincidence window as:

$$N_{CC}(\tau) = AP(k = 0)f(\tau)\left[g_0(\tau - Z) + g_0(\tau) + g_0(\tau + Z)\right]$$

$$N_{AC}(\tau) = A\sum_{k=1-N}^{k=1+N} P(k \neq 0)f(\tau)\left[g_k(\tau - Z) + g_k(\tau) + g_k(\tau + Z)\right]$$

Where A is a proportionality constant. We also introduced a noise term, which is given by $N_{noise}(\tau)$:

$$N_{noise}(\tau) = Af(\tau)b$$

Let $z \in (-Z, 0, Z)$ and $\gamma = \frac{m+1}{m}$. Finally, the model for the number measured coincidence $N(\tau)$ is given by:

$$\begin{aligned}N(\tau) &= N_{CC}(\tau) + N_{AC}(\tau) + N_{noise}(\tau) \\ &\approx Af(\tau)m^2\eta^2\left(\frac{m+1}{m}\sum_z g_0(\tau + z) + \sum_{k\neq 0}\left((N - |k|)\sum_z g_k(\tau + z)\right) + b\right) \\ N(\tau) &\approx A'f(\tau)\left(\gamma N\sum_z g_0(\tau + z) + \sum_{k\neq 0}\left((N - |k|)\sum_z g_k(\tau + z)\right) + b\right) \qquad (1)\end{aligned}$$

III. RESULTS

A. Spatial Distribution for the measured coincidence of Two Rings Metasurface experiment

The experimental setup for the two rings experiment is illustrated in Fig. 2. Continuous-Wave (CW) laser is used to produce photons for the experiment, and ND filter is used to reduce the intensity of the laser to fulfil the low-light condition for the photon interference. The laser is split into two paths with the same distance (delay line set to the balancing position) by using a Polarized Beam Splitter (PBS), namely the SLM path (upper right) and reference path (bottom left). The SLM path will pick up a random phase factor from the SLM. The two paths will be recombined on the second beam splitter with orthogonal polarization, in this case no interference occurs as the photons from the two paths are distinguishable. The beam is passed to the two-overlapping-rings metasurface sample with angle of $\pm 22.5^{\circ}$ and a vertical analyzer before measured by the SPAD camera, which is configured with 2 µs frame time and 500 ms aquisition time, i.e. 250000 frames in total.

The experimental result showing the spatial distribution of the measured coincidence using nearby pixel filter with $r = 2$ and $t_{cc} = 4$ is shown in Figure 3. Figure 3(a) shows the coincidence map when only reference path is incident, where the right ring is bright. Figure 3(b) shows the coincidence map when only SLM path is incident, where the left right is bright. Figure 3(c) shows the result when both paths are incident, where both rings are bright, and (d) shows the result after averaging bad pixels with the adjacent pixels.

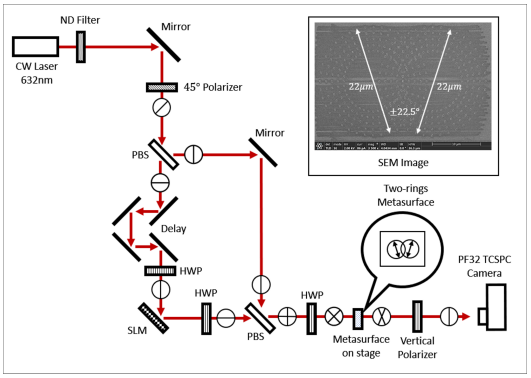

FIG. 2. Continuous-Wave (CW) laser is used to generate photons with low intensity. The first PBS is used to split the laser into two paths with different polarization. The SLM path (bottom left) is set at the balancing position relative to the reference path (top right). The two path is recombined at the second PBS, interferes on the two rings metasurface and measured by the SPAD camera. The circles denote the laser polarization. Top right image shows the SEM image of the two-overlapping rings metasurface sample.

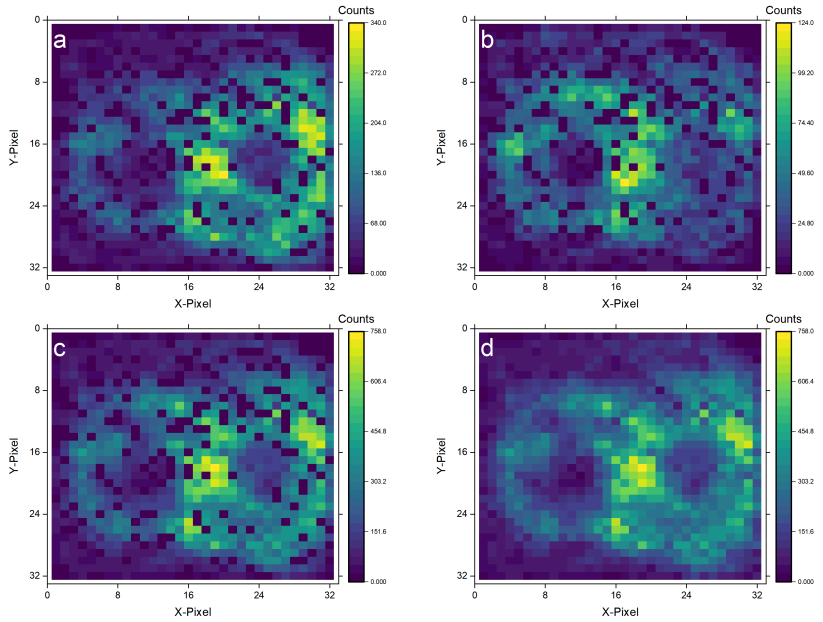

FIG. 3. The spatial distribution of the two rings metasurface experiment with verital polarizer by using nearby filtering pixel, with $r = 2$, (a) only reference path incident, (b) only SLM path incident, (c) both path incident, and (d) both paths incident after averaging the bad pixels with the adjacent pixels

B. Temporal distribution of the measured coincidence of fine scan experiment

The experimental setup of fine scan experiment is shown in Fig 4. The delay line will scan around the balancing position of the two paths and extract the temporal distribution of the measured coincidence discussed in the Section II.A, and we will fit the model discussed in the Section II.B to see how the model fits with the measured coincidence. While the SPAD camera specification suggests that there are $Z = 1024$ time bins, we can see from the Fig 4.b that the total the effective number of time bins is only $Z = 922$. The camera is configured with 5 µs frame time and 250 ms aquisition time, i.e. 50000 frames in total, and the camera uses $N = 100$ cycles per frame. The measured jitting time between the camera and the laser is $\Delta T \approx (184.318 \pm 0.001)$ ps and the measured laser FWHM is $t_w \approx (185.4 \pm 1.6)$ ps. The expected number of detection per pixel per frame in our experiment is $\eta \sim 0.003$.

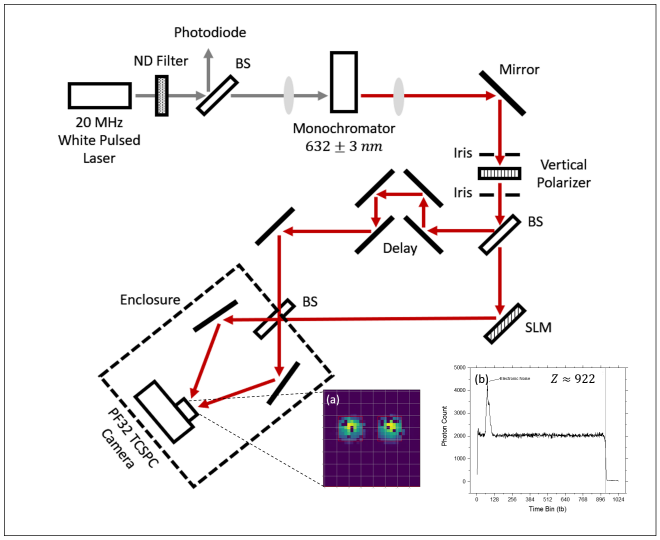

FIG. 4. Continuous-Wave (CW) laser is used to generate photons with low intensity. The laser is split into two paths, reference and delay paths, and recombined in the second BS where the two-photons interference occurs when the two paths are at balanced position. The PF32 SPAD camera is used to time tag the arrival time of each photons. (a) shows the two spots of the accumulated photon count per pixel, and (b) shows the accumated photon count per time bin, note that the effective time bin $Z \approx 922$ instead of 1024 due to electronical defect.

The measured coincidence and the model result is shown in Fig 5 (top). First, we can note some features of the measured coincidence:

- sloped-triangle in the center
- one peak on top of the sloped-triangle
- two side peaks

The model suggests that the only the center peak on top of the sloped triangle is the contribution of the true coincidence, and the sloped-triangle and the two side peaks is the contribution of the accidental coincidence. With setting $N = 100$ and $t_{cc} = 4$ tb, the fitting result at the balancing position is:

$$\begin{aligned}
\gamma &= 1.693 \pm 0.019 \\
\Delta T &= (3.456 \pm 0.004)\,\text{tb} \\
t_w &= (3.35 \pm 0.13)\,\text{tb} \\
\tau_0 &= (0.00 \pm 0.06)\,\text{tb} \\
A' &= 216.8 \pm 0.4 \\
b &= 10.21 \pm 0.29 \\
Z &= (922.6 \pm 0.5)\,\text{tb}
\end{aligned}$$

Where 1 tb = 53.42 ps is the time bin size of our SPAD camera. Note that ΔT and t_w agree with out measurement results.

To obtain the true coincidence from the measured coincidence, we subtract the measured coincidence with our model accidental coincidence and noise. The result of after the accidental coincidence and noise subtraction is shown on Fig 5 (bottom). After extracting the true coincidence, we can take the center datapoints from $-t_{cc}/2$ to $+t_{cc}/2$, to extract the quantum coincidence from the two-photons interference effect. Fig 6 shows the HOM dip of the true coincidence, which is obtained by subtracting the measured coincidence with the model accidental count and noise.

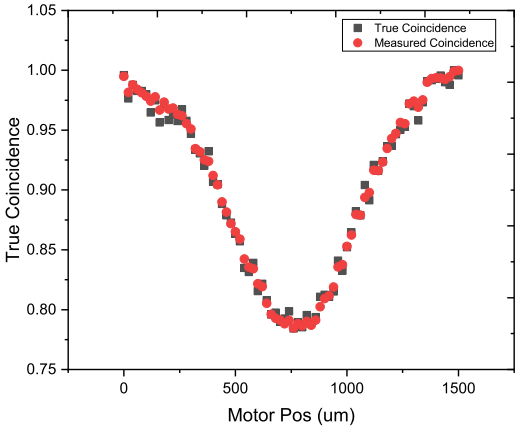

FIG. 6. HOM dip of the normalized true coincidence and normalized measured coincidence vs. delay position, the result suggests that the true coincidence and accidental coincidence are proportional, i.e. $\gamma \sim 1.693$ is constant for all delay positions.

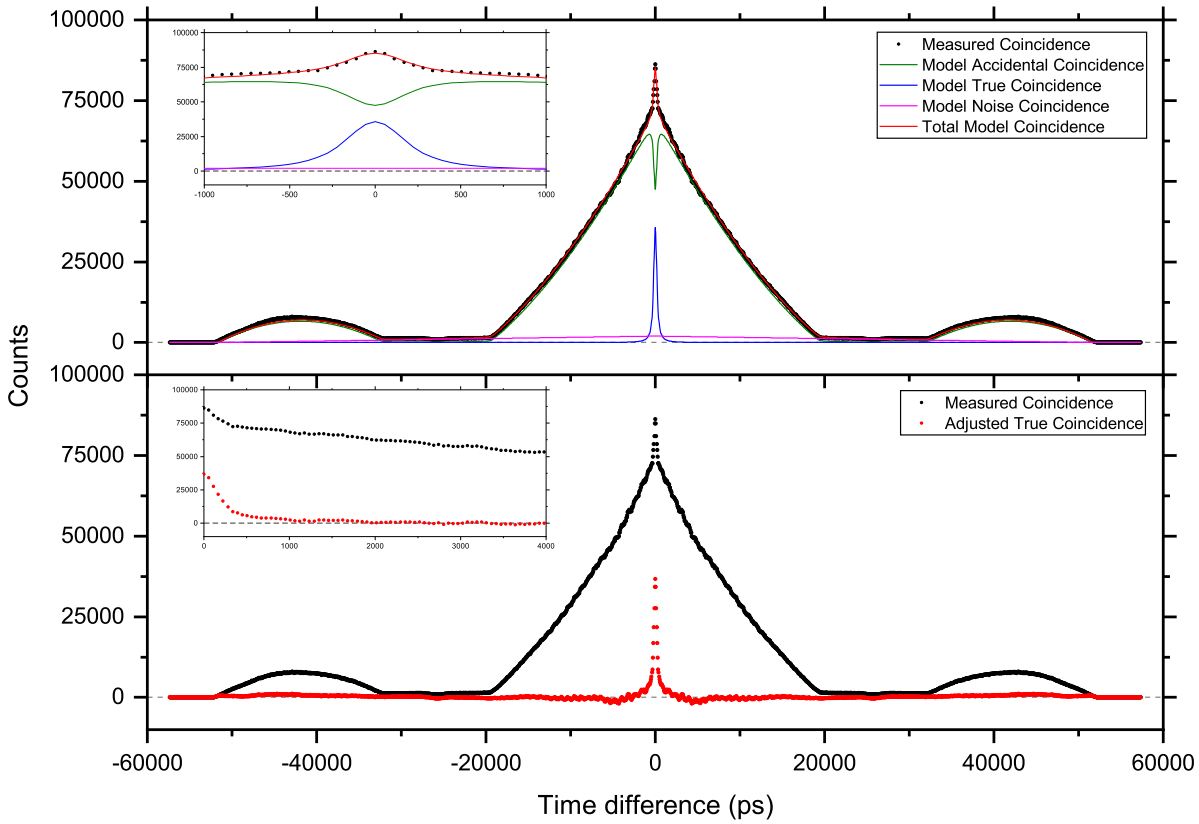

FIG. 5. [top] The measured coincidence (black) and the fitting model (red) comparison. The model fitting can be decomposed into true coincidence (blue), accidental coincidence (green), and noise (magenta). [bottom] The adjusted true coincidence (red) after subtracting the measured coincidence (black) with the model accidental count and noise.

IV. DISCUSSION

For the metasurface sample experiment, currently, we are using vertical analyzer angle. It is possible to extend the experiment by observing how the spatial distribution of the coincidence changes with the analyzer angle. This topic will be further discussed in the future work.

For the fine scan experiment, we have shown that the model works really well to predict the temporal distribution of the measured coincidence. However, there are still some unanswered questions regarding the results, such as (1) why the ratio of the true coincidence and the measured coincidence is constant for different delay line positions, and (2) why the accidental coincidence also varies with the delay position. We predicted that using the model will yield improvement on the HOM dip depth, but in this case, we did not see any depth improvement. One possible cause is that the model is still incomplete at predicting the two photons interference effect. This topic will be further discussed in the future work.

V. CONCLUSION

In this work we demonstrated the capabilities of 32x32 pixels picosecond time resolved SPAD camera. This allows us to measure the spatial and temporal distribution of the photon coincidence. We proposed a fully vectorized algorithm to efficiently count both spatial and temporal distribution of the coincidence of any pixel regions, which will be very useful in future experiments and analysis in terms of optimizing the storange and running time of the data analysis. Furthermore, we also derived a model to explain the temporal distribution of the coincidence, in which the measured coincidence is decomposed into true coincidence, accidental coincidence, and noise. Finally, we also show the two-photons interference/HOM dip of the true coincidence derived from our model.

[1] R. A. Shelby, Experimental verification of a negative index of refraction, Science **292**, 77 (2001).

[2] J. B. Pendry, Negative refraction makes a perfect lens, Physical Review Letters **85**, 3966 (2000).

[3] D. Schurig, J. J. Mock, B. J. Justice, S. A. Cummer, J. B. Pendry, A. F. Starr, and D. R. Smith, Metamaterial electromagnetic cloak at microwave frequencies, Science **314**, 977 (2006).

[4] M. Unternahrer, B. Bessire, L. Gasparini, D. Stoppa, and A. Stefanov, Coincidence detection of spatially correlated photon pairs with a monolithic time-resolving detector array, Optics Express **24**, 28829 (2016).

[5] B. Eckmann, B. Bessire, M. Unternahrer, L. Gasparini, M. Perenzoni, and A. Stefanov, Characterization of space-momentum entangled photons with a time resolving cmos spad array, Optics Express **28**, 31553 (2020).

[6] S. P. Poland, N. Krstajic, J. Monypenny, S. Coelho, D. Tyndall, R. J. Walker, V. Devauges, J. Richardson, N. Dutton, and P. e. a. Barber, A high speed multifocal multiphoton fluorescence lifetime imaging microscope for live-cell fret imaging, Biomedical Optics Express **6**, 277 (2015).

[7] G. Satat, M. Tancik, O. Gupta, B. Heshmat, and R. Raskar, Object classification through scattering media with deep learning on time resolved measurement, Optics Express **25**, 17466 (2017).

[8] G. Gariepy, N. Krstajic, R. Henderson, C. Li, R. R. Thomson, G. S. Buller, B. Heshmat, R. Raskar, J. Leach, and D. Faccio, Single-photon sensitive light-in-fight imaging, Nature Communications **6**, 10.1038/ncomms7021 (2015).

[9] R. S. Tanuwijaya, T. K. Yung, and J. Li, Measurement of speed of light by coincidence count method (2020).

[10] S. Cova, M. Ghioni, A. Lacaita, C. Samori, and F. Zappa, Avalanche photodiodes and quenching circuits for single-photon detection, Applied Optics **35**, 1956 (1996).